

Adsorption of Dihydrogen on Mesoporous Materials at 77 K

V. Yu. Gavrilov

Boreskov Institute of Catalysis, Siberian Division, Russian Academy of Sciences, Novosibirsk, 630090 Russia

Received December 18, 2003

Abstract—The adsorption of dihydrogen at 77 K is studied on a series of oxide materials including silica, pure titania and alumina, and mixed oxides. The experimental data obtained suggest that the sorption properties per unit area of mesopore surface depend on both the texture and chemical composition of the sample. A comparative procedure for the analysis of dihydrogen adsorption isotherms is considered.

The study of the physical adsorption of dihydrogen has a long history that has mainly dealt with microporous adsorbents. For example, the possibility of the separation of hydrogen isotopes by means of sorption on synthetic zeolites has recently attracted great attention [1–3]. Currently, the physical adsorption of hydrogen on carbon as well as on non-carbon disulfide nanotubes, zeolites, fullerenes, and other microporous materials is considered promising for the storage of dihydrogen, an environmentally friendly energy source [4–8].

At the same time, the physical adsorption of H_2 can be used as a method for the investigation of the structure of ultramicroporous materials, owing to the extremely small kinetic size of the hydrogen molecule ($\sigma_k = 0.289 \text{ nm}$ [9]) and the absence of activated diffusion in micropores at 77 K. The applicability of the comparative method of H_2 adsorption isotherm analysis to the study of the ultramicroporous texture of activated carbons and zeolites was demonstrated in [10, 11]. However, the possible influence of the fine structure and chemical nature of the mesopore surface on the results of the comparative analysis remains unclear.

This work is aimed at a refinement of the methodology and field of application of the comparative processing of hydrogen adsorption isotherms for disperse materials with various textural and chemical compositions.

EXPERIMENTAL

Hydrogen adsorption isotherms were measured at 77 K on a DigiSorb-2600 Micromeritics (the United States) automated setup. The range of sorbate pressures was 1–100 kPa. Samples were pumped at 300°C for 5 h immediately before adsorption runs.

The following oxide materials were examined: silica with a regular hexagonal structure (MCM-41) [12]; fine-mesopore silica materials named SM-1 and SM-2; typical mesoporous specimens of SiO_2 , Al_2O_3 , and TiO_2 ; and the mixed mesoporous thermal oxides $ZrO_2 + Al_2O_3$ and $ZrO_2 + TiO_2 + SnO_2$. The table presents the main

textural parameters of these materials derived from low-temperature nitrogen adsorption isotherms: S_α (m^2/g) is the specific surface area determined by the conventional comparative method [13]; V_s (cm^3/g) is the limiting volume of the sorption space; and C_{BET} is the energy constant of the BET equation. The equivalent pore-size distribution of pore volume was estimated by the Barrett–Joyner–Halenda (BJH) method [14] from the desorption branch of the nitrogen adsorption isotherm.

RESULTS AND DISCUSSION

Figures 1 and 2 show experimental H_2 adsorption isotherms for oxide materials. Similar dark and light points represent adsorption and desorption equilibria, respectively. Clearly, adsorption and desorption are completely reversible and adsorption capacity varies considerably from sample to sample.

None of the samples contains true micropores, as can be seen from the values of C_{BET} , from the comparative plots of nitrogen adsorption isotherms, and from differential pore size distribution (Fig. 3). Study of the adsorption of N_2 , O_2 , and Ar vapors on the finest pore

Textural parameters of oxide materials derived from N_2 sorption isotherms at 77 K

Material	S_α , m^2/g	V_s , cm^3/g	C_{BET}
MSM-41	1195	1.141	75
SM-1	637	0.589	87
SM-2	1034	0.596	70
SiO_2	334	0.925	102
Al_2O_3	230	0.695	105
$ZrO_2 + Al_2O_3$	133	0.223	80
TiO_2	124	0.377	80
$ZrO_2 + TiO_2 + SnO_2$	72	0.200	102

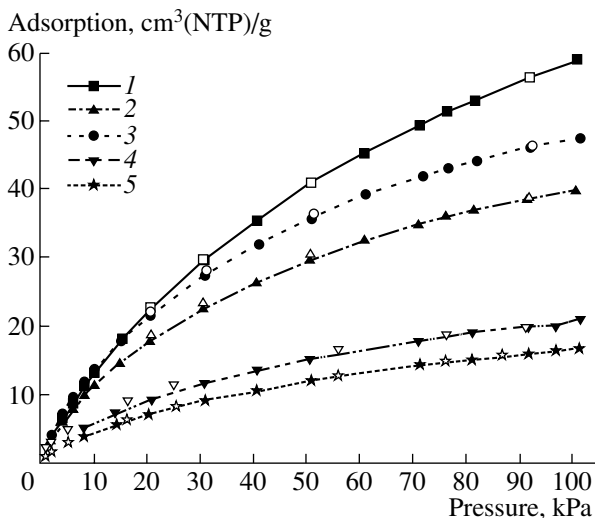


Fig. 1. Hydrogen adsorption on (1) MCM-41, (2) SM-1, (3) SM-2, (4) SiO_2 , and (5) Al_2O_3 at 77 K.

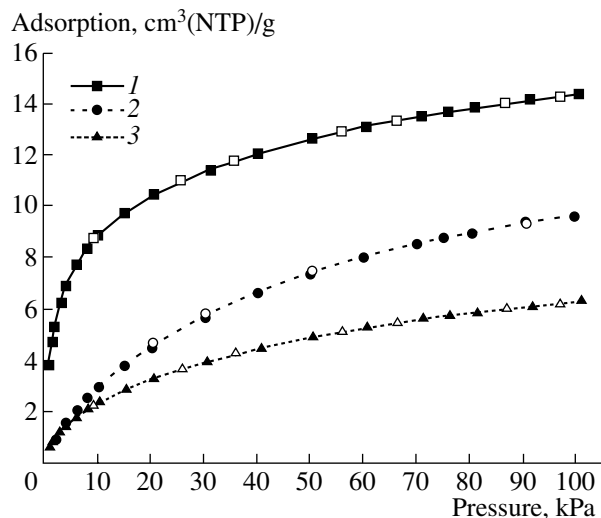


Fig. 2. Hydrogen adsorption on (1) TiO_2 , (2) $\text{ZrO}_2 + \text{Al}_2\text{O}_3$, and (3) $\text{ZrO}_2 + \text{TiO}_2 + \text{SnO}_2$ at 77 K.

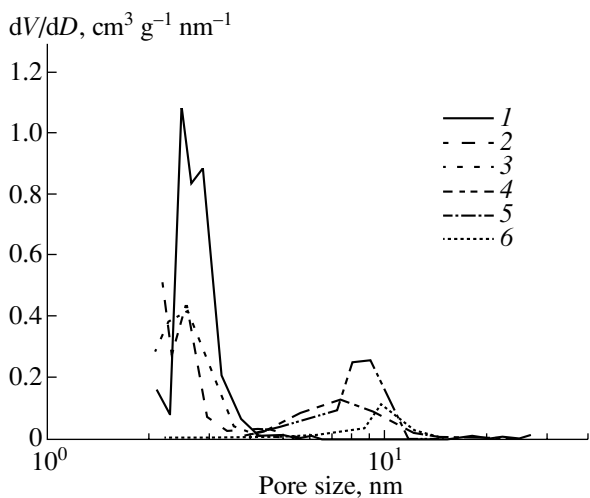


Fig. 3. Differential pore-size distribution for (1) MCM-41, (2) SM-1, (3) SM-2, (4) SiO_2 , (5) Al_2O_3 , and (6) TiO_2 .

materials—MCM-41, SM-1, and SM-2 [15]—demonstrated that the pore structure of these materials is mainly fine mesoporous, with a narrow size distribution. Therefore, hydrogen adsorption capacity $A(P)$ is determined, in the first approximation, by the accessible surface area: $A(P) \approx \alpha(P)S_\alpha$ (the variable $\alpha(P)$ reflects the structure of the sorption layer and accounts for the possible effect of the chemical composition of the surface on this structure).

Figure 4 presents absolute H_2 sorption isotherms ($A(P)/S_\alpha = f(P)$) for some oxides as well as data for meso-macroporous carbon black with a specific surface area of $90 \text{ m}^2/\text{g}$ [11]. In this case, isotherms are again different. This is due to the dependence of the sorption

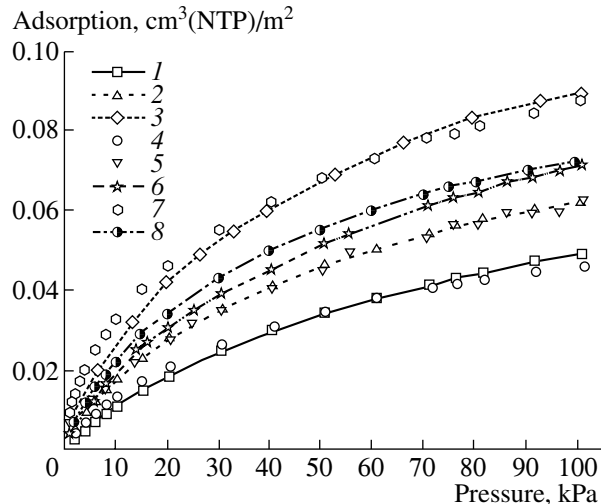


Fig. 4. Absolute hydrogen adsorption isotherms for (1) MCM-41, (2) SM-1, (3) carbon black [11], (4) SM-2, (5) SiO_2 , (6) Al_2O_3 , (7) $\text{ZrO}_2 + \text{TiO}_2 + \text{SnO}_2$, and (8) $\text{ZrO}_2 + \text{Al}_2\text{O}_3$.

layer structure on surface properties rather than to the geometric difference between the samples.

Hydrogen adsorption capacity at 77 K is not high in the pressure range examined and can be attributed only to some fraction of the “dense sorption monolayer,” a_m . Indeed, formal estimates based on data from [13, 16] demonstrate that the maximum adsorption capacity of the carbon material at 100 kPa (Fig. 4)—this is $0.09 \text{ cm}^3 \text{ (NTP)}/\text{m}^2$ and is equivalent to 2.4 molecules of H_2 per square nanometer under the assumption that hydrogen molecules are spherical, have a size of $\sigma_k = 0.289 \text{ nm}$, and are randomly and densely packed into a two-dimensional monolayer—is at most $(0.3\text{--}0.4) a_m$. This parameter is substantially lower for the other

materials. For MCM-41 and SM-2, which are characterized by the lowest sorption capacity, it is equal to 1.3 molecule H₂ per square nanometer or $\sim 0.2 a_m$.

It is believed that the H₂ adsorbed on the mesopore surface at 77 K (supercritical temperature) is mobile and nonlocalized and that adsorption tends to the value characteristic of a monolayer as the pressure is raised. To describe these sorption processes, several theoretical models based on the state equation were elaborated, which were summed up and compared, for example, in [17, 18]. They allow one to correlate, with different degrees of reliability, the surface coverage with the equilibrium sorbate pressure and to predict two-dimensional phase transitions under certain conditions. One of these models is given by the well-known Hill-de Boer isotherm equation [19].

Examination of the mobile adsorption models [19, 20] suggests that critical phenomena in the sorption layer occur below the critical temperature at pressures ensuring a coverage of at least 0.33 and alter the shape of the adsorption isotherm, bringing about typical S-like inflections. From the adsorption conditions in our experiments and from the shape of isotherms being qualitatively invariable, we infer that the adsorbed H₂ is a two-dimensional gas on the mesopore surface. If the observed adsorption is significantly higher than the adsorption typical of nonlocalized sorption per unit mesopore area or the shape of the isotherm is markedly different, as in the case of TiO₂ (Fig. 2), then other sorption processes have likely occurred in parallel.

An empirical additive scheme of hydrogen sorption on materials containing ultramicropores, true micropores, and developed mesoporous texture was proposed in [11]. It is accepted in that scheme that adsorption processes on these structural elements occur independently. Under this assumption, the sorption isotherm equation can be written as:

$$A(P) = A^0 + V_\mu^0 \beta(P) + S_\alpha \alpha(P), \quad (1)$$

where A^0 (cm³ (NTP)/g) is specific adsorption (for example, on Lewis and other surface sites [21, 22]) plus adsorption in the ultramicropores, that is, the pores accessible only to hydrogen molecules (it is assumed that the ultimate adsorption A^0 is achieved at the minimum hydrogen pressure and does not change as the pressure is elevated); $\alpha(P)$ (cm³(NTP)/m²) is adsorption per unit area of the mesopore surface; V_μ^0 is the volume of the true micropores; and $\beta(P)$ (cm³(NTP)/cm³(pores)) is hydrogen adsorption per unit volume of true micropores.

It is clear from relationship (1) that $A(P)$ depends on two independent variables, $\alpha(P)$ and $\beta(P)$, which can be reliably determined only experimentally and only for chemically similar samples that are differentiated by adsorption taking place mainly on the mesopore surface or in the volume of true micropores. However, relationship (1) is not restricted to any particular range

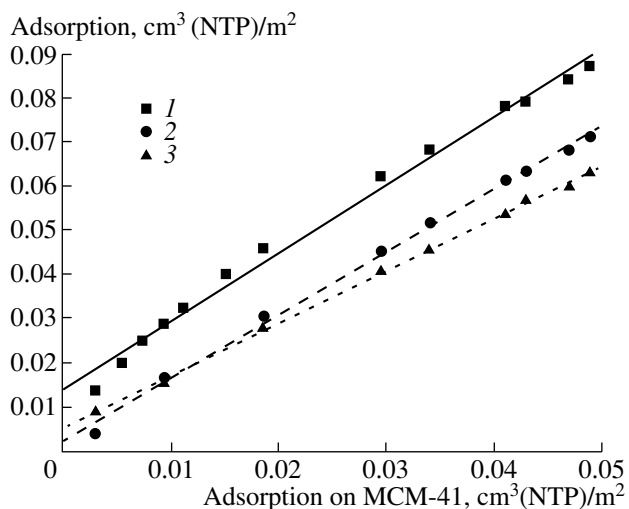


Fig. 5. Absolutr hydrogen adsorption on (1) ZrO₂ + TiO₂ + SnO₂, (2) Al₂O₃, and (3) SiO₂ at 77 K relative to than on MCM-41.

of sorbate pressures and, accordingly, to any degree of filling of the sorption space.

The method of the comparative processing of hydrogen adsorption isotherms proposed in [11] implicitly introduces some *a priori* simplifications: it is assumed that $\alpha(P)$ depends weakly on the chemical nature and structure of the mesopore surface and that typical microporous materials (such as zeolite ZSM-5 [10]) are characterized by the same $\beta(P)$ value. Under these assumptions, relationship (1) takes the form

$$A(P) - S_\alpha \alpha(P) = A^0 + V_\mu^0 \beta(P), \quad (2)$$

and the comparative plot is described by $A(P) - S_\alpha \alpha(P) = f(\beta(P))$. For materials with developed microtexture, such as activated carbons, the contribution from sorption on the mesopore surface should be taken into account only if $S_\alpha > 80-100 \text{ m}^2/\text{g}$. Otherwise, the contribution from $S_\alpha \alpha(P)$ can be neglected, as in the case of zeolites and related materials with a small external surface area of crystallites (aggregates).

However, as can be seen from Fig. 4, the fact that $\alpha(P)$ is independent of the chemical nature and/or structure of the surface layer is not obvious. It is only evident that the absolute value of sorption decreases with increasing the specific surface area.

In Fig. 5, we compare absolute H₂ sorption isotherms measured at the same sorbate pressure for MCM-41 (material with the greatest specific surface area of mesopores and the lowest sorption capacity) and a number of other adsorbents, namely, the mixed thermal oxide ZrO₂ + TiO₂ + SnO₂ and mesoporous Al₂O₃ and SiO₂. Figure 6 shows a similar comparison including data for SM-1. The isotherms that coincide numerically with the “references” chosen are omitted.

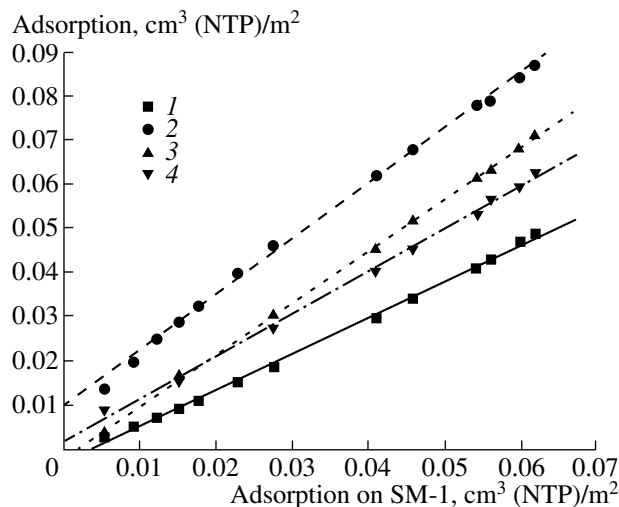


Fig. 6. Absolute hydrogen adsorption on (1) MCM-41, (2) $\text{ZrO}_2 + \text{TiO}_2 + \text{SnO}_2$, (3) Al_2O_3 , and (4) SiO_2 at 77 K relative to that on SM-1.

It is clear from the above figures that most of the isotherms are affine to the reference isotherms in a wide pressure range. At the same time, the ordinate intercept can be either positive or negative and the slope can be either above or below unity. The totality of these facts are evidence of a proportional change in the sorption properties of a unit surface area (in the density of the two-dimensional sorption layer) relative to the reference sample in a wide range of sorbate pressures (where the plots are linear). In the first case, only an increase in the density of the sorption layer takes place, showing itself as the slope of the relative adsorption plot increasing by a factor of 1.53 for $\text{ZrO}_2 + \text{TiO}_2 + \text{SnO}_2$ and by a factor of 1.17 for SiO_2 . For the second series of materials (Fig. 6), the relative density of the sorption layers can either increase or decrease: it is 0.82 for MCM-41, 1.25 for $\text{ZrO}_2 + \text{TiO}_2 + \text{SnO}_2$, and 0.97 for SiO_2 . Hence, the data obtained are *relative* in nature.

The variability of the sorption properties per unit area of mesopore surface is likely to be due to the fact that adsorbents differ in the energy of sorption interaction between H_2 molecules and the surface layer, resulting in different heats of adsorption. The main component of the intermolecular interaction in the case of mobile sorption is collective dispersion interaction, whose strength (U) is determined as the sum of elemental pair interactions between sorbate molecules and surface atoms: $U \approx \sum^n \epsilon(x)$ [14, 18]. If there are no reliable experimental data, it can be deduced from general considerations that the heat of physical adsorption of H_2 on the surface of mesoporous materials at 77 K is not high. As a consequence, even a slight change in its absolute value can be a powerful driving force in the structural transformation of the sorption layer. Let us consider possible causes of the variation of the energy

of interaction between the sorbate and mesopore surface.

The above-mentioned finding that the absolute value of hydrogen sorption decreases with increasing specific surface area suggests the following inference: as the size of the smallest texture element (thickness of the pore wall for MCM-41 and SM specimens or the size of a primary particle for the corpuscular materials Al_2O_3 and SiO_2) decreases, the number of the surface atoms (n) occurring in the nearest environment of the sorbate molecule and participating in the pair dispersion interaction decreases and, therefore, so does the total energy of intermolecular adsorption interaction.

Analyzing the pure geometric aspect of the problem that is illustrated by Fig. 4, one should not ignore the chemical nature of the adsorbent surface. The energy of intermolecular interaction between the sorbate and surface is determined by their individual properties and is qualitatively described [18] by the expression

$$\epsilon(x) \approx -\frac{\delta_1 \delta_2}{x^6 \left(\frac{1}{\hbar v_1} + \frac{1}{\hbar v_2} \right)},$$

where subscripts 1 and 2 stand for sorbate molecules and surface, δ is polarizability, and $\hbar v$ is the characteristic energy, which can be taken to be roughly equal to the ionization energy.

The intrinsic polarizability of molecules is an additive property of all structural elements, atoms and bonds [23]. In turn, the polarizability of the surface molecules of an adsorbent (δ) is determined by the bulk properties of the adsorbent phase. According to the Clausius–Massotti equation [24], $\delta \approx (M/\rho)(\epsilon - 1)/(\epsilon + 2)$, where M is the molecular weight, ρ is density, and ϵ is dielectric permeability. According to reference data [25], the polarizabilities of SiO_2 and carbon are 6.0 and 0.9 \AA^3 , respectively. These values, considered as rough estimates, indicate that the adsorbents differ essentially in the energy of pair intermolecular interaction with the same sorbate. In this case, it is the chemical nature of the adsorbent surfaces that is responsible for the unproportional change in the sorption and geometric properties of the sorbents.

Therefore, the use of the “universal” values of $\alpha(P)$ in constructing comparative plots in terms of relationship (2) requires caution. When there is uncertainty in setting the parameter $\alpha(P)$, the developed mesopore surface can introduce an error in the interpretation of the comparative plots. By way of example, let us apply comparative analysis to TiO_2 , whose isotherm has an unusual shape (Fig. 2) as compared to the other samples.

Figure 7 compares H_2 adsorption isotherms for TiO_2 with absolute adsorption isotherms for MCM-41 and SM-1 in terms of expression (1), taking into account that there are no micropores in the titania sample and, accordingly, the $V_\mu^0 \beta(P)$ term is absent. The plots are

linear in a wide range of surface coverages, and their slopes are equal and correspond to a titania surface area of $129 \text{ m}^2/\text{g}$; this finding is in good agreement with nitrogen adsorption data (see the table).

At the same time, the ordinate intercepts are evidence of the presence of texture regions that are filled with hydrogen by a mechanism independent of the mesopore surface area. The specific sorption A^0 (relative to the references chosen) takes different values of ~ 6.8 and $8.1 \text{ cm}^3 \text{ (NTP)}/\text{g}$. It is believed that this specific component is primarily due to sorption, at the lowest pressures, in ultrafine pores accessible to hydrogen molecules but inaccessible to the larger molecules of nitrogen ($\sigma_k = 0.364 \text{ nm}$ [9]). The strict reversibility of the adsorption isotherms, which would not be observed for H_2 chemisorption on selective surface sites, is evidence in favor of the sorption nature of this component. The fact that the different reference isotherms lead to different values of relative specific sorption is likely to be due to the presence of ultrafine pores in SM-1. It is believed that use of the data obtained for MCM-41 or of the very similar data for SM-2 as the reference isotherm will allow one to judge whether a material examined shows specific sorption. In this case, one will obtain a result that is very close to the absolute value (i.e., the value that would be observed in the absence of specific adsorption sites in the reference sample).

Indeed, the mesopore surface area of $\sim 1100 \text{ m}^2/\text{g}$ in the oxide materials corresponds to the minimum possible particle size of the oxide phase or to the minimum pore wall thickness in the case of the regular hexagonal structure of MCM-41. Hence, one can expect that the absolute hydrogen sorption capacity (in view of its trend shown in Fig. 4) will also be the lowest for this surface area. At the same time, the probability of specific sorption due to the molecular-sieve properties of the textural elements with the smallest volume becomes minimal. In view of this, the averaged H_2 sorption isotherm for MCM-41 and SM-2 at 77 K in the pressure range 1–100 kPa, which is suitable for comparative analysis, can be represented as an interpolation polynomial adequately fitted to the experimental data:

$$\begin{aligned} \alpha = & 3.088 \times 10^{-4} + 1.56 \times 10^{-3}P - 4.927 \times 10^{-5}P^2 \\ & + 1.283 \times 10^{-6}P^3 - 1.932 \times 10^{-8}P^4 \\ & + 1.478 \times 10^{-10}P^5 - 4.457 \times 10^{-13}P^6 \text{ cm}^3 \text{ (NTP)}/\text{m}^2, \end{aligned}$$

where P is the equilibrium pressure, kPa.

Therefore, the comparative processing of hydrogen adsorption isotherms at 77 K differs from the conventional methods of the comparative analysis of vapor (e.g., nitrogen) adsorption isotherms. In the case of nitrogen, the polymolecular-sorption portion of the isotherm is usually examined, where the sorbate–sorbent interaction is not specific and the sorbate–sorbate interaction is prevailing. The approach suggested here allows the *absolute* geometric parameters of texture (surface areas of the meso- and macropores and the micropore volume) to be calculated. H_2 adsorption at

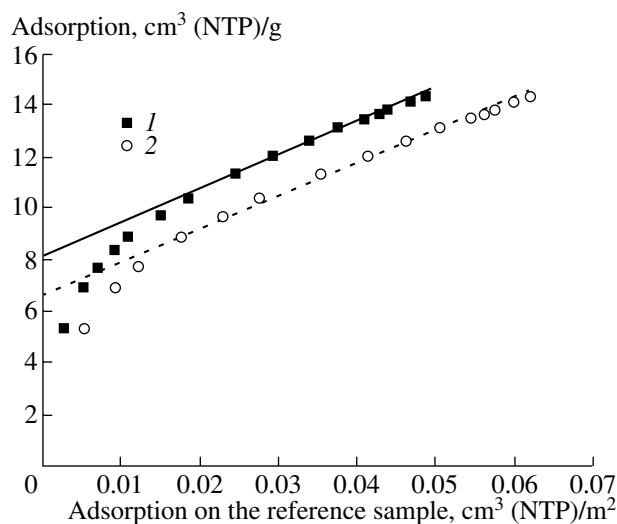


Fig. 7. Comparison of the H_2 adsorption isotherm for TiO_2 with the absolute adsorption isotherms for (1) MCM-41 and (2) SM-1 at 77 K.

supercritical temperatures and pressures below 100 kPa is limited to the initial stage of monolayer filling, at which the surface sorption properties are very sensitive to the structure and chemical composition of the surface. Therefore, if the comparative analysis of adsorption isotherms in terms of relationship (2) involves a contribution from sorption on developed mesopore surface, one can obtain only a *relative* result and, accordingly, relative values of textural parameters.

REFERENCES

1. Panchenkov, G.M., Tolmachev, A.M., and Zolotova, T.V., *Zh. Fiz. Khim.*, 1964, vol. 38, no. 8, p. 1361.
2. Kocherukhin, V.E. and Zel'vinskii, Ya.D., *Zh. Fiz. Khim.*, 1964, vol. 38, no. 10, p. 2594.
3. Parbuzin, V.S., Panchenkov, G.M., Rakhamukov, B.Kh., and Sandul, G.V., *Russ. J. Phys. Chem.*, 1967, vol. 41, no. 1, p. 193.
4. Darkrim, F. and Levesque, D., *J. Phys. Chem. B*, 2000, vol. 104, no. 29, p. 6773.
5. Kawamura, Y., Konishi, S., and Nishi, M., *J. Nucl. Sci. Technol.*, 2000, vol. 37, no. 6, p. 536.
6. Ye, Y., Ahn, C.C., Fultz, B., Vajo, J.J., and Zinck, J.J., *Appl. Phys. Lett.*, 2000, vol. 77, no. 14, p. 2171.
7. Ivanitskii, A.L., *Usp. Khim.*, 2002, vol. 71, no. 3, p. 203.
8. Chen, J., Kuriyama, N., Yuan, H., Takeshita, H.T., and Sakai, T., *J. Am. Chem. Soc.*, 2001, vol. 123, no. 47, p. 11 813.
9. Breck, D., *Zeolite Molecular Sieves: Structure, Chemistry and Use*, New York: Wiley, 1974.
10. Gavrilov, V.Yu., *Kinet. Katal.*, 1995, vol. 36, no. 4, p. 631.
11. Gavrilov, V.Yu., *Kinet. Katal.*, 1995, vol. 36, no. 5, p. 787.

12. Beck, J.S., Vartulli, J.C., Roth, W.J., Leonowicz, M.E., Kresge, C.T., Schmitt, K.D., Chu, C.T.-W., Olson, D.H., Sheppard, E.W., McCullen, S.B., Higgins, J.B., and Schlenker, J.L., *J. Am. Chem. Soc.*, 1992, vol. 114, no. 27, p. 10 834.
13. Karnaukhov, A.P., *Adsorbsiya. Tekstura dispersnykh i poristykh materialov* (Adsorption: Texture of Disperse and Porous Materials), Novosibirsk: Nauka, 1999.
14. Gregg, S.J. and Sing, K.S.W., *Adsorption, Surface Area and Porosity*, London: Academic, 1982.
15. Gavrilov, V.Yu., *Kinet. Katal.* (in press).
16. Zagrafskaya, R.V., Karnaukhov, A.P., and Fenelonov, V.B., *React. Kinet. Catal. Lett.*, 1981, vol. 16, no. 1, p. 233.
17. Jaycock, M.J. and Parfitt, G.D., *Chemistry of Interfaces*, New York: Wiley, 1981, p. 279.
18. Adamson, A.W., *Physical Chemistry of Surface*, New York: Wiley, 1976, p. 520.
19. De Boer, J.H., *The Dynamical Character of Adsorption*, Oxford: Oxford Univ. Press, 1968, p. 132.
20. Broekhoff, I.S.P. and van Dongen, P.H., *Physical and Chemical Aspects of Adsorbents and Catalysts*, Linssen, B.G., Ed., London: Academic, 1970, p. 67.
21. Kustov, L.M., Alekseev, A.A., Borovkov, V.Yu., and Kazanskii, V.B., *Dokl. Akad. Nauk SSSR*, 1981, vol. 261, no. 6, p. 1374.
22. Kazansky, V.B., *J. Catal.*, 2003, vol. 216, nos. 1–2, p. 192.
23. Vereshchagin, A.N., *Polyarizuemost' molekul* (Polarizability of Molecules), Moscow: Nauka, 1980.
24. Ashcroft, N.W. and Mermin, N.D., *Solid State Physics*, New York: Holt, Rinehart & Winston, 1976, vol. 2.
25. *Spravochnik khimika* (Chemist's Handbook), Leningrad: Khimiya, 1971, vol. 1; *Fizicheskie velichiny: Spravochnik* (Physical Quantities: A Handbook), Moscow: Energoatomizdat, 1991.